

Home / Archives / Vol. 20 No. 4 (2025)

Vol. 20 No. 4 (2025)

Published: 2025-08-01

Editorial Piece

Challenges, Innovations, and Future Directions in Life Cycle Assessment of Product and Process Impacts

Nicolás Martín Clauser, Maria Cristina Area

8392-8395

PDF

The Sometimes Antisocial Nature of Nanofibrillated Cellulose and Some Other Papermaking Fiber Surfaces

Martin A. Hubbe

8396-8399

PDF

Research Article or Brief Communication

Artificial Neural Network Approach for Predicting Enzymatic Hydrolysis of Steam Exploded Pine Wood Chip in Mild Alkaline Pretreatment

Hyeon Cheol Kim, Si Young Ha, Jae-Kyung Yang

8400-8419

PDF

How Can Regional Cultural Symbols be Integrated into Public Seating Design? An Innovative Exploration Using Marbled Porcelain Patterns as an Example

Jixiao Chang, Hongbin Han, Kai Yuan

8420-8438

PDF

Relationship Between Wood Specific Gravity and Average Annual Ring Width of 15 Korean Wood Species

Kug-Bo Shim, Min-Soon Park, Yonggun Park, Chul-Ki Kim, Hyun Mi Lee

8439-8455

PDF

Numerical Simulation of Stress Wave Propagation in the Three-Layer Medium Structure of Standing Trees

Yingchun Gong, Jialei Qu, Haiqing Ren, Shubing Chen, Fenglu Liu

8456-8472

PDF

3D-Printed Green Biocomposites from Poly(lactic acid) and Pine Wood-derived Microcrystalline Cellulose: Characterization and Properties

Selwin Maria Sekar, Rajini Nagarajan, Ponsuriyaprakash Selvakumar, Nadir Ayrlimis, Kumar Krishnan, Faruq Mohammad, Hamad A. Al-Lohedan, Sikiru O. Ismail

8473-8492

PDF

Comparative Analysis of Fiber Characteristics and Chemical, Physical, and Mechanical Properties of Six Indigenous Bamboo Species from Indonesia

Sarah Augustina, Riana Anggraini, Ika Yuliandari, Antalina Florida br Marpaung, Feby Savva Charisma, Muhammad Rasyidur Ridho, Pati Kemala, Seng Hua Lee, Apri Heri Iswanto, Petar Antov, Widya Fatriasari

8493-8514

PDF

**Response Mechanism of Extracellular Laccase Activity of *Lyophyllum decastes* to Cultivation Substrates and Subculture**

Xue Xiong, Peng Li, Wei Li, Gui-he Zhang 8515-8527



**Sustainable Gift Packaging Design Based on KANO-AHP-QFD**

Jiajia Fan, Wei Wang 8528-8550



**Structural Behavior of Beam-to-Column Glued Laminated Timber Connection Using Double Steel Plates**

Yosafat Aji Pranata, Bambang Suryatmono, Rohana Hassan, Olga Catherina Pattipawaej, Zakiah Ahmad 8551-8565



**A Multi-Criteria Decision-Making Framework for Tibetan Furniture Design Driven by the Needs of Users: Integration and Evaluation via TFAHP-QFD-VIKOR**

Xinlian Li, Jing Wang, Ning Tang 8566-8590



**Mechanical and Thermal Behavior Analysis of Chicken Feather/*Sesbania grandiflora* Fibers-based Hybrid Epoxy Composites**

Shankar Kannan Paramasivam, Muthukannan Marimuthu, Arun Sakthivel, Janani Rajasekar, Sivasubramanian Palanisamy, Kuwar Mausam, Aravindhan Alagarsamy, Quanjin Ma, Saleh A Al-Farraj 8591-8610



**Generative Design of Bamboo Furniture Combining Game Theory and AI-Generated Content**

Jing Liu, Honghe Gao, Olga Yezhova 8611-8631



**Finite Element Analysis of Structural Safety and Support Reinforcement Efficacy in a Large Old Zelkova Tree: A Case Study of a Natural Monument**

Sung-Jun Pang, Ji Sun Jung, Gwang Gyu Lee, Jin Ho Shin, Ji Won Son 8632-8653



**Dual Role of *Pennisetum purpureum* as a Phytogenic Feed Additive: Enhancing Growth and Profitability in Antibiotic-Free Broiler Production**

Alvin Lim Teik Zheng, Kelly Kai Seng Wong, Yee Lyn Ong, Jacqueline Lease, Yoshito Andou, Faez Firdaus Abdullah Jesse, Eric Lim Teik Chung 8654-8673



**Effect of Sal Wood and Babool Sawdust Fillers on the Mechanical Properties of Snake Grass Fiber-Reinforced Polyester Composites**

Giridharan Ravichandran , Karuppasamy Ramasamy , Karuppusamy Manickaraj, Sathish Kalidas, Manivannan Jayamani, Kuwar Mausam, Sivasubramanian Palanisamy, Quanjin Ma, Saleh A Al-Farraj 8674-8694



**Sustainability Potential and Utilization of Agricultural Bioenergy in Turkey**

Dursun Kemal Bayraktar 8695-8712



**Effect of Fe (III) Addition on Ammonium Loss and Associated Microbial Gene Expression in Soils**

Liyu Cheng, Hongjie Zhu, Weihao Xing, Benjun Zhou 8713-8724



**High-Strength UV-Resistant Polyvinyl Alcohol Composite Films Based on *Phellodendron amurense* Rupr Extract**

Feng Li, Hongpeng Li, Guo Li, Yujia Zhang, Haoyu Ma, Min Tang 8725-8736



**Influence of Bamboo Cellulose Coating on the Flux Performance of Polyvinylidene Fluoride Hollow Fiber Membrane**

Perry Law Nyuk Khui, Md Rezaur Rahman, Khairul Anwar bin Mohamad Said, Murtala Namakka, M. Shahabuddin, Muneera S. M. Al-Saleem, Jehan Y. Al-Humaidi, Mohammed M. Rahman, King Kuok Kuok 8737-8754



<b>Following a Self-guided Trail within an Accredited US Campus Arboretum: The Use of an AI-based App for Tree Identification and Tour Enrichment</b>	
Merve Kalaycı Kadak	8755-8776
<a href="#">PDF</a>	
<b>Techno-Economic Analysis of Lignin-Containing Micro- and Nano-Fibrillated Cellulose for Lightweight Linerboard Packaging</b>	
Heather Starkey , Maria Gonzalez , Hasan Jameel, Lokendra Pal	8777-8790
<a href="#">PDF</a>	
<b>One-Step Alkaline-Hydrogen Peroxide Degumming of Hemp Fiber: Optimization for Enhanced Processability and Eco-Efficiency</b>	
Huanghuang Chen, Zhen Wang, Bo Jiang, Mingfang Liu, Huanghuang Chen, Bifeng Luo, Wenxiang Hong	8791-8810
<a href="#">PDF</a>	
<b>Application of Paulownia Wood Based on Fuzzy Theory Decision-Making</b>	
Xiaohan Shen, Junzhe Liu, Yixian Xiao, Xinyuan Shao, Xiaoli Zou	8811-8840
<a href="#">PDF</a>	
<b>The Evolution and Impact of Furniture Design in Contemporary Society</b>	
Burcin Saltik	8841-8847
<a href="#">PDF</a>	
<b>Measurement and Optimization of Wood Dust and Noise Levels in Table Saw Operations Using Response Surface Methodology</b>	
Özcan Gül, Mustafa Korkmaz	8848-8862
<a href="#">PDF</a>	
<b>Performance Evaluation of Coconut Wood Veneer Composite for Sustainable Construction Material</b>	
Shamil Haque Kizhakkethodi Mansoor , Vishnu Raju, Anish Mavila Chathoth, Shibu Comath, Adiyodi Venugopal Santhoshkumar, Sreejith Babu, Pavin Praize Sunny, Arjun Memuttathu Sajeevan	8863-8882
<a href="#">PDF</a>	
<b>Reinforcement of Paper Documents by Different Starch Modification Processes</b>	
Jing Lang	8883-8898
<a href="#">PDF</a>	
<b>Research on Function-Interface Design of Old and Antique Hongmu Furniture E-commerce Platform in the Second-hand Economy Environment</b>	
Yuhan Li, Yu Feng, Lei Fu, Jiufang Lv	8899-8924
<a href="#">PDF</a>	
<b>Particleboard Surface Optimization for High-Quality Laminating with Decor Paper</b>	
Coskun Kursun, Saadettin Murat Onat, Orhan Kelleci, Suheyila Esin Koksall	8925-8948
<a href="#">PDF</a>	
<b>Structural Toughness Enhancement Method for Material Extrusion-Based 3D-Printed Model: A Rigid Shell-Flexible Infill Composite Structure</b>	
Chen Wang, Han-yi Huang, Xiaowen Wang	8949-8956
<a href="#">PDF</a>	
<b>Harvest Process Analysis and Damage Evaluation of Longitudinal Roller Type Corn Picker</b>	
Rongjian Tai, Jianjun Guo, Jiwang Zhang, Fanyeqi Yang, Fengchi Wang, Jiansheng Gao, Guosong Liu, Dongbo Zhao	8957-8975
<a href="#">PDF</a>	
<b>Laminated Wood Material Reinforced with Bacterial Cellulose Sheets Derived from Kombucha Pellicles: Part 1 — Some Physical Properties</b>	
Mehmet Budakçı, Diğdem Şağban, Mustafa Korkmaz, İzham Kılınc	8976-8992
<a href="#">PDF</a>	
<b>Enhanced Retention, Durability, and Strength of Old Corrugated Containers With Water-Borne Polyurethane (Water-Borne PU)</b>	

**Enhanced Retention, Drainage, and Strength of Old Corrugated Container Pulp Using Poly(aluminum chloride), Nanofibrillated Cellulose, and Hydrophobic Colloidal Silica Particles**

Seyed Ali Askarabadi, Mohammad Talaeipour , Hossein Jalali Tarshizi , Amirhooman Hemmasi 8993-9007



**Bridging Time: A Dual Path Analysis of Chinese Furniture Culture from Diplomatic Exchange to Digital Narratives**

Liang Xu, Rong Wei, Xinyou Liu 9008-9019



**Phytochemical Characterization of Cleome droserifolia Biomass and its Application as in vitro Antioxidant, Anti-Inflammatory, Anti-Diabetic, and Anti-Yeast Agents**

Mohamed Abdel-Aal Amin, Mahmoud H. Hendy, Sulaiman A. Alsalamah , Salma Yousif Sidahmed Elsheikh, Ahmad M. Abdel-Mageed, Shereen Ahmed Elwasefy, A. M. Elbasiony, Ismail M. A. M. Shahhat 9020-9032



**Integrated Analysis of Cork Presence in Korean Oak Barks Using Visual Inspection, Colorimetry, FT-IR, and Py-GC/MS**

Byeongho Kim, Kyoung-Chan Park, Denni Prasetya, Jong-Ho Kim, Nam-Hun Kim, Xuanjun Jin, Joon Weon Choi, Se-Yeong Park 9033-9050



**Exploring the Relationship between Visual Evaluation and User Preference in Wooden Cork Flooring: An Application of the Semantic Differential Method**

Meng Zhu, Dietrich Buck; Bo Shen; Zhaolong Zhu 9051-9062



**Fabrication of Poly(lactic acid) Microspheres with Various Micro-Structure by Microfluidic T-junction and Gelatin Pore-forming Agent**

YanJun Bai, Feng Liu, Yifan Zhang, Lei Wu, Haihu Liu, Yan Ba 9063-9078



**Changes of Soil Organic Carbon Stabilization and Stock in Yancheng Huang-Bohai Sea Migratory Bird Habitat Coastal Marsh Wetland with a Long-term Follow-up Study**

Chaowei Yue, Yun Zhu, Haochuan Ge, Hui Wang, Guixiang Quan, Liqiang Cui, Jinlong Yan 9079-9102



**Extreme Gradient Boosting Model to Predict Antioxidant Activity of Extract from Ainsliaea acerifolia**

Hyeon Cheol Kim, Woo Seok Lim, Si Young Ha, Jae-Kyung Yang 9103-9126



**Biotic Stress Responses and Oxidative Defense Mechanisms of Pinus brutia against Pine Processionary Moth Infestations**

Ergin Yilmaz , Esra Nurten Yer Çelik, Orhan Gulseven , Şeyma Selin Akin, Nezahat Turfan, Sezgin Ayan 9127-9147



**Synthesis of CuO Nanoparticles Using Waste-Derived Bamboo Cellulose for Enhanced Catalytic and Antibacterial Applications**

Alvin Lim Teik Zheng, Sarah Sabidi , Melissa Alexander Maran, Kar Ban Tan , Kelly Kai Seng Wong, Eric Lim Teik Chung, Yoshito Andou 9148-9166



**Effects of Different Visual Styles on Elderly Users’ Interaction Behavior in Smart Sofa Interfaces**

Jiayu Tang, Xinghao Liu, Chengmin Zhou, Jake Kaner 9167-9183



**Composites with Recovered Polystyrene Reinforced with Pine or Poplar Residues Following Lignin Extraction**

Orhan Kelleci 9184-9207



**Paper Fingerprint by Forming Fabric: A Univariate Feature Selection Approach Using Periodic Marks Analysis**

Yong Ju Lee, Chang Woo Jeong, Tai-Ju Lee, Geon-Woo Kim, Hyoung Jin Kim 9208-9225






**Lignin Reattachment to Pulp Fibres During Brownstock Washing: The Role of Sodium Sulfate**

Eashwara Raju Senthilkumar, Veerababu Poliseti, Tomas Vikström, Gunnar Henriksson, Olena Sevastyanova


9226-9241

 PDF

**Influence of Pulp Temperature and Convective Drying on Wet Tensile Strength of Towel Papers with Poly(amidoamine epichlorohydrin) Additive**

Mariusz Reczulski, Piotr Pospiech, Bogumiła Delczyk-Olejniczak, Maria Biełkowska


9242-9256

 PDF

**Enhancing Polyester Composites with Nano Aristida hystrix Fibers: Mechanical and Microstructural Insights**

Pitchai Pandiarajan, Padamathur Ganesan Baskaran , Sivasubramanian Palanisamy, Manickaraj Karuppusamy, Kathiresan Marimuthu, Anish Rajan, Mansour I. Almansour, Quanjin Ma, Saleh A Al-Farra


9257-9281

 PDF

**The Sensual Intention of Wardrobe Furniture Materials Based on Women’s Visual and Tactile Experience Evaluation**

Jingyu Sun, Wei Wang


9282-9295

 PDF

**Suppression of NF κB p65 and STAT3 by Melicope pteleifolia Extract Mitigates Ovalbumin Driven Allergic Rhinitis in Mice**

Aling Zhang, Jialiu Ji, Jiani Wu, Jin Liu, Shuangjian Wu


9296-9311

 PDF

**The Khene: A Lao Mouth Organ of the Isan Region of Thailand**

Ahmad Faudzi Musib, Aaliyawani Ezzerin Sinin, Sinin Hamdan, Khairul Anwar Mohamad Said, Ezra Alfandy M. Duin


9312-9331

 PDF

**Comparative Evaluation of Hydrodistillation, Supercritical Fluid Extraction, and Organic Solvent Extraction on Leaf Essential Oils of Chamaecyparis formosensis and C. obtusa var. formosana and Their Potential as Wood-Protective Agents**

Ying-Ju Chen, Fu-Lan Hsu, Sen-Sung Cheng


9332-9347

 PDF

**Hyperproduction and Characterization of a Cost-Effective Manganese Peroxidase from Pleurotus ostreatus Using Response Surface Methodology under Solid State Fermentation**

Tahreem Nasir, Zafar Iqbal, Hafsa Tariq, Zahid Anwar, Muhammad Nadeem Zafar, Muhammad Zubair, Sajjad Hussain Sumrra, Muddassar Zafar


9348-9376

 PDF

**Nail-holding Capacity of Guiding Bore Hole Diameter in P. massoniana and C. lanceolata Dimension Lumber**

Jiankun Liang, De Li, Linjing Lan, Haiyuan Yang, Xin He, Yu He, Yuqi Yang, Cheng Li, Zhigang Wu


9377-9389

 PDF

**Pulp Production from Pineapple Leaf Waste for Sustainable Paper Manufacturing**

Md. Didarul Alam Chowdhury, Ektiar Uddin, Muhammad Misbah Uddin, Rehan Hasnain, S.M. Mehedi Afnan Rejve, Md Shiman Rusdi, Md Rezaur Rahman, Muneera S. M. Al-Saleeme, Jehan Y. Al-Humaidi, Mohammed M. Rahman


9390-9405

 PDF

**A Case Study on Sonic Heritage and Acoustic Profiling of the Bamboo Bass Guitar**

Ahmad Faudzi Musib, Aaliyawani Ezzerin Sinin, Sinin Hamdan, Khairul Anwar Mohamad Said, Khairil Anwar Dean Kamarudin


9406-9423

 PDF

**Mechanism of Ink and Pigment Detachment from Palm Leaf Manuscripts Driven by Hygroexpansion**

Xingling Tian, Pei Hu

9424-9437

 PDF

**Activated Carbon Coating Films from Renewable Resources: Advancing Eco-Friendly Food Packaging**

Redzuan Mohammad Suffian James, H'ng Paik San, Norwahyuni Mohd Yusof, Seng Hua Lee

 PDF

**Research Progress of Finite Element Technology in Wood Processing**

Maosen Wang, Lin Yang

 PDF

**Bacterial Cellulose: A Novel Antibacterial Material for Biomedical Applications, Wound Healing, and Sustainable Infection Control**

Samy Selim, Mohammad Harun-Ur-Rashid , Yousef Alhaj Hamoud, Hiba Shaghaleh , Mohammed S. Almuhayawi, Mutasem S. Almehayawi, Soad K. Al Jaouni

 PDF

**Environmentally Friendly Composites from Agricultural Residue Biomass for Lightweight Applications in New Generation Structures: A Review**

Murugesan Palaniappan, Sivasubramanian Palanisamy, Borhen Louhichi, Nadir Ayrlimis, Thulasi mani Murugesan

 PDF

**Ionic Liquids as an Effective Medium for Enzymatic Saccharification of Lignocellulosic Biomass: A Review**

Wen Jun Dong, Li Shuang Wang, Dan Rui Wang, Shi Jia Dong, Zhi Yuan Xu, Xiao Mei Hu

 PDF

# Structural Behavior of Beam-to-Column Glued Laminated Timber Connection Using Double Steel Plates

Yosafat A. Pranata <sup>a,\*</sup> Bambang Suryoatmono <sup>b</sup> Rohana Hassan <sup>c</sup>,  
Olga C. Pattipawaej <sup>a</sup> and Zakiah Ahmad <sup>c</sup>

The structural performance of timber buildings is significantly affected by the behavior of connections. This study investigated the structural behavior of bolted glulam beam-to-column connections with external steel plates. Data were obtained for the structural behavior of two types of connections. The glulam was manufactured from Red Meranti (*Shorea* spp.). The load-carrying capacity, moment capacity, rotational stiffness, initial stiffness, post-elastic stiffness, and ductility ratio of the connections were evaluated and discussed. The results indicate that the type 1 connection was in the partial ductility capacity category ( $\mu = 2.60$ ), while the type 2 connection was in the limited ductility ( $\mu = 1.27$ ). The average moment capacities of type 1 and type 2 connections were 4.56 kN.m and 21.2 kN.m, respectively. The moment and rotation relationships models of the glulam beam-column were approximately bilinear with initial stiffness 9 times and 2.4 times for type 1 and type 2 connections, respectively, compared to corresponding post-elastic stiffness. Steel plates helped improve ductility ratio, as shown by splitting failures near the column bolt rows. This stiffness model can then be used as input data for spring properties of similar connections in the analysis of multi-story building structures.

DOI: 10.15376/biores.20.4.8551-8565

*Keywords:* Glulam; Beam-to-column connection; Moment capacity; Stiffness; Ductility ratio

*Contact information:* a: Master Program in Civil Engineering, Maranatha Christian University, Jl. Suria Sumantri 65, Bandung, 40164, West Java, Indonesia; b: Doctoral Program in Civil Engineering, Parahyangan Catholic University, Jl. Ciumbuleuit 94, Bandung, 40161, West Java, Indonesia; c: School of Civil Engineering, Universiti Teknologi MARA, 40450 UiTM Shah Alam, Selangor, Malaysia;

\* Corresponding author: yosafat.ap@maranatha.ac.id

## INTRODUCTION

Glued laminated timber (glulam) is a widely used engineered wood product designed for structural applications, particularly in multi-story and long-span construction. Its high strength-to-weight ratio, dimensional stability, and design flexibility make it an ideal choice for modern timber structures. Within such structural systems, the beam-to-column connection plays a pivotal role, significantly affecting the overall load transfer and lateral stiffness. The strength and stiffness behavior and reliability of these connections are therefore critical to ensuring the performance and integrity of the entire timber structure. Many glulam joints, especially those with dowels, bolts, or glued-in rods, show brittle failure modes. Enhancing ductility without sacrificing strength remains a challenge.

Multi-story glulam timber buildings utilizing moment-resisting frame systems can exhibit ductile structural behavior, provided that the beam-to-column connections are capable of ductile performance. Such ductility ratio ensures structural resilience in regions with moderate to high seismic risk. Several studies have explored mechanical fasteners and steel plate reinforcements as connection elements, showing the potential to enhance beam-to-column joints' stiffness and overall performance in glulam structures. Furuheim and Nesse (2020) studied the effect of gusset plates and found that they not only increased moment resistance but also led to more consistent and predictable failure patterns, enhancing the safety and reliability of timber connections. He *et al.* (2020) proposed using knee braces to improve the performance of bolted glulam beam-to-column connections, which typically have low rotational stiffness. Their results showed that knee braces significantly increased joint rigidity, load capacity, and rotational performance, effectively changing the connection from semi-rigid or flexible to a more rigid and reliable form.

Yang *et al.* (2021a) examined the static and seismic performance of two glulam connection types: a basic screw-only setup and an improved version with added steel brackets. While the screw-only connections offered moderate strength and stiffness, the steel brackets greatly enhanced the connection's behavior. They improved load distribution, delayed brittle failure, and increased energy dissipation during cyclic loading, making the joint more ductile and resilient. Yang *et al.* (2021b) conducted experimental tests to investigate the behavior of beam-to-column glulam connections with screwed-in threaded rods. The parameters studied are failure modes, moment resistance, initial rotation stiffness, ductility ratio, and energy dissipation capacity.

Ottenhaus *et al.* (2021) outlined design strategies for achieving ductility ratio in timber connections, particularly those using dowel-type fasteners under lateral loads. They highlighted that, because timber tends to be brittle in tension and shear, the connections themselves are often the main source of ductility ratio and energy dissipation. The study supports using performance-based design to ensure ductile behavior. Guo *et al.* (2022) studied energy-dissipative connections in timber frames, showing that steel reinforcement can significantly improve performance. Similarly, Wang *et al.* (2023) investigated semi-rigid timber joints with embedded steel parts, finding they offered better load transfer and deformation capacity than traditional fasteners.

Many studies support the advancement of hybrid or reinforced connection systems to improve the performance of glulam structures. For example, Li *et al.* (2021) investigated two types of beam-to-column connections: one using double external steel plates and another with a single embedded steel plate. Both setups were tested with bolts and screws. The results showed that both configurations improved joint performance, with the double steel plate setup offering higher moment resistance and better energy dissipation. The embedded plate also reduced slip and provided more consistent rotational behavior.

Reboucas *et al.* (2022) reviewed ductile moment-resisting connections for timber frames and found that reinforced bolted slotted-in steel plates and glued-in steel rods significantly improved rotational capacity and energy dissipation, making them suitable for multi-story timber buildings in seismic areas. Ductility ratio classes for connections are classified into four categories (Reboucas *et al.* 2022), which are brittle ductility ratio ( $\mu \leq 2$ ), low or partial ductility ratio ( $2 < \mu \leq 4$ ), moderate ductility ratio ( $4 < \mu < 6$ ), and high ductility ratio ( $\mu \geq 6$ ).

Hubbard and Salem (2024) examined four types of moment-resisting glulam beam-to-column connections using fastened steel rods. All types showed ductile behavior before failure, with gradual strength reduction and good deformation capacity. Amrudin *et al.* (2024) conducted an experimental study to assess the bolt-bearing strength and withdrawal resistance of glulam elements, offering valuable insights into how glulam connections perform mechanically. This research supports the safe and effective use of glulam in modern structural applications.

These studies above highlight the need to design timber connections that can withstand inelastic deformations without losing strength. As glulam is increasingly used in multi-story and long-span buildings, ductile connection systems are crucial for enhancing structural resilience and energy dissipation. The use of mechanical connectors and steel plates improves the strength and stiffness behaviors of the connections.

In Indonesia, the use of glulam has grown significantly due to rising demand for sustainable building materials and the development of local manufacturing facilities. However, to support broader use of glulam made from Indonesian tropical timber in residential and commercial projects, more comprehensive data on mechanical properties and connection performance are needed. Currently, such data are limited and not yet adequate for standardized structural design. This study investigates the structural performance of glulam beam-to-column connections for two-story wooden frame buildings using glulam manufactured from Indonesian tropical hardwood timber.

The glulam structure consists of beams supported at each end by columns or other main beams (Swedish Wood 2024a). For small spans, beams of prismatic section are often preferable. For larger spans, the non-prismatic sectional depth should vary with the internal forces in the beam (Swedish Wood 2024b). Figure 1 shows the typical connection types in a framed structure (Swedish Wood 2024b), where 1 is a column-base connection, 2 is a beam-column connection, 3 is a beam-to-beam connection, 4 is column top-beam connection, 5 is a beam joint, 6 and 7 are tie fixing. Joints are weak parts in timber frame buildings, often determining the bearing capacity of the entire structure. Joints for glulam are often based on steel plates and dowels.

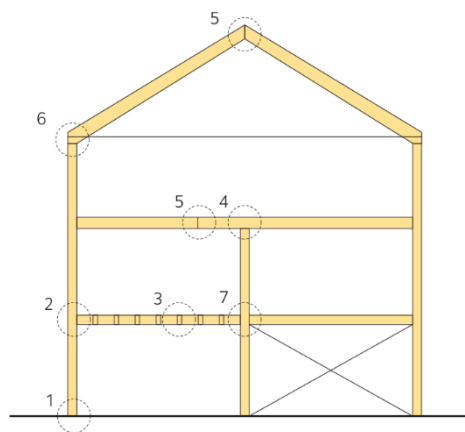


**Fig. 1.** Typical connection types in a framed structure (Swedish Wood 2024b)



## EXPERIMENTAL

### Preparation of Specimens

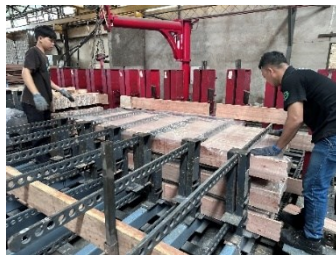
The glulam beam specimens used in this study were manufactured from Red Meranti (*Shorea* spp.), a tropical hardwood species commonly found in Indonesia. A local glulam manufacturing facility produced the glulam members using standard industrial procedures. The adhesive employed in the lamination process was phenol resorcinol formaldehyde (PRF), a durable, water-resistant adhesive known for its strong bond performance in structural applications.



(a) Finger-jointed lamella



(b) Finger-joint



(c) Clamping process



(d) Glulam beams

**Fig. 2.** The glulam manufacturing process

The manufacturing process began with the visual grading of the sawn timber to ensure consistency in quality and strength. Following grading, the timber pieces were prepared for finger jointing, where lamella ends were cut into interlocking profiles (Fig. 2a) to be joined together to form finger jointed lamella (Fig. 2b). The next step involved the application of PRF adhesive to the bonding surfaces of the planed lamella. The lamella with face gluing was then arranged in layers on a clamping bed and subjected to uniform pressure using a hydraulic or mechanical clamping system to ensure full contact and bonding across all layers (Fig. 2c). The glulam beams were constructed using four (4) and six (6) laminations, with each lamella having a thickness of 31 mm. After adequate curing, the laminated timber was removed from the press, cut to the required dimensions, and conditioned for testing. The prepared glulam beam specimens ready for structural testing are shown in Fig. 2d.

This study focused on two types of beam-to-column glued laminated timber connections. The first configuration (Type 1) features a connection between the glulam beam and column members, with 90 mm × 126 mm cross-sectional dimensions. The glulam elements are composed of four laminae, each with a thickness of 31 mm. The second configuration (Type 2) is also a beam-to-column connection, where the beam and column members have cross-sectional dimensions of 90 mm × 210 mm. This glulam section consists of six laminae, each 31 mm thick. The specific gravity of glulam is 0.542



(Pranata *et al.* 2025a). Type 1 and Type 2 connections were assembled using 12-mm diameter bolts, with 5-mm-thick steel plates positioned on either side of the joint, as illustrated in Figs. 3 and 4, respectively. Pranata *et al.* (2024, 2025b) have tested the tensile properties of bolts with the results of 355 MPa ( $F_y$ ) and 388 MPa ( $F_u$ ). Testing the flexural yield strength ( $F_{yb}$ ) of bolts has also been previously conducted by Pranata *et al.* (2011, 2013) with results of 632. MPa. Pranata *et al.* (2024, 2025b) have conducted experimental testing of the tensile properties of steel plates with the results of 318 MPa ( $F_y$ ) and 422 MPa ( $F_u$ ). The number of bolts used for each connection type is detailed in Table 1. Three replicate specimens were prepared for each type of connection. Murtopo *et al.* (2020) have tested the physical and mechanical properties of glulam made of Red Meranti wood with the results of specific gravity of 0.5 and modulus of elasticity of 10370 MPa.

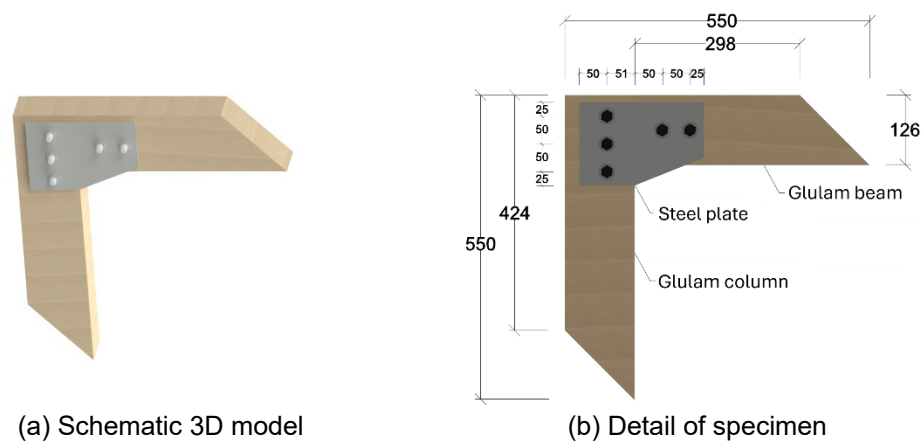


**Fig. 3.** Glulam beam-to-column connection, Type 1 (all dimensions are in mm)

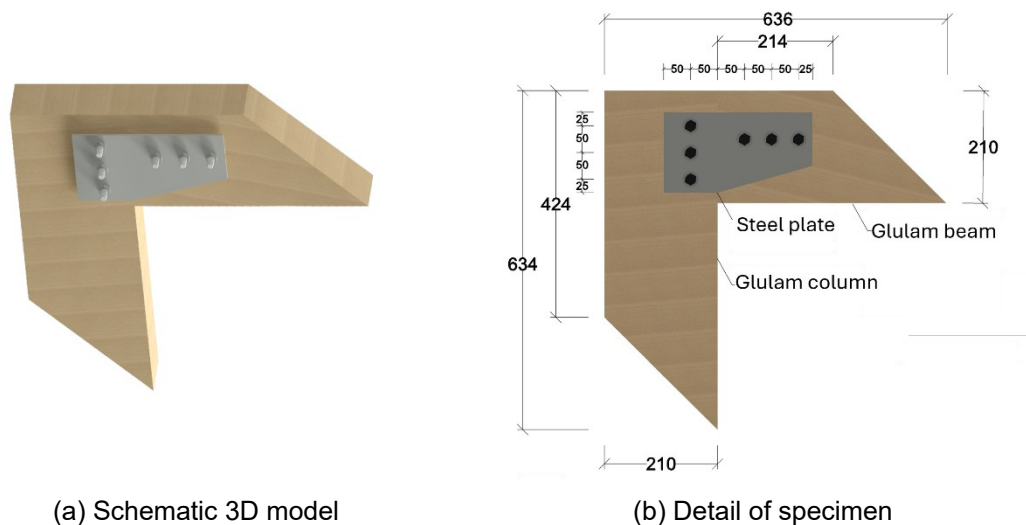


**Fig. 4.** Glulam beam-to-column connection, Type 2 (all dimensions are in mm)

**Table 1.** Specification of Type 1 and Type 2 Glulam Beam-to-Column Connections

Specimen	Beam Cross-section	Column Cross-section	Number of Laminae	Number of Bolts in the Beam	Number of Bolts in Column	Number of Specimens
Type1	90 x 126 mm	90 x 126 mm	4	2	3	3
Type2	90 x 210 mm	90 x 210 mm	6	3	3	3

These two types of joints were studied in this research, with the consideration of studying the behavior of connections included in the brittle ductility ratio category (Type 2) and the low or partial ductility ratio category (Type 1).

### Test Methods

The connection tests were conducted using a Universal Testing Machine HT-9501 with a maximum capacity of 1000 kN, operating under displacement control mode. All testing procedures adhered to the guidelines specified in EN 26891 (1991), with a constant displacement rate of 3.2 mm/min. The specimens were positioned between the loading head and platform to apply compressive force to the connection, as illustrated in Fig. 5.

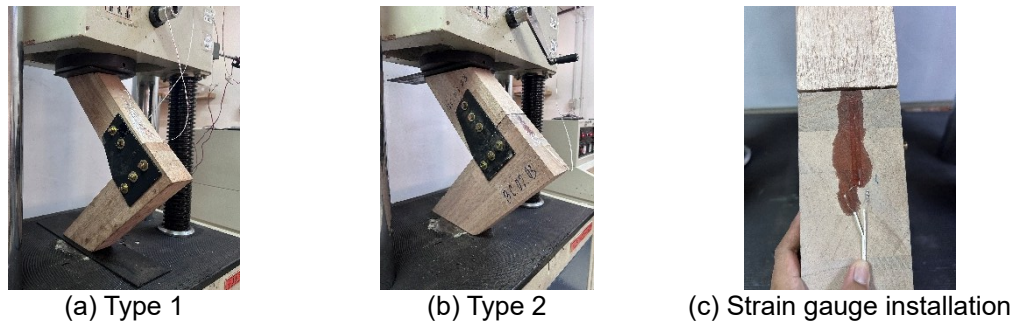
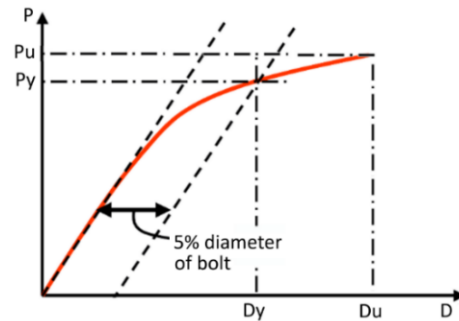
**Fig. 5.** Test setup of glulam beam-to-column connections for Type 1 and Type 2

Figure 5a shows the test setup for the Type 1 beam-to-column connection specimen, and Fig. 5b illustrates the test setup for the Type 2 beam-to-column connection specimen. Meanwhile, Fig. 5c, shows strain gauges installed on the column cross-section for both Type 1 and Type connections, aimed at investigating strain variations caused by splitting, thereby providing empirical data on the strain history in the column bolt row. Throughout the testing, load and displacement data were recorded and subsequently analyzed to obtain the necessary parameters, namely load carrying capacity, moment capacity, rotational stiffness, initial stiffness, post-elastic stiffness, and ductility ratio.

Pozza *et al.* (2023) demonstrated that the experimental capacity curve of steel-to-timber connections generally does not show a well-defined yielding limit, suggesting that variations in yielding behavior must be considered during design considerations. Hence, the 5%-offset diameter method identifies the yield point by considering a specific offset in the load-deformation curve, effectively indicating a material's transition from elastic to post-elastic behavior.



**Fig. 6.** The method to determine the yield points (ASTM D5764 2018)

For this study, the determination of the joint capacity of the glulam beam-to-column connection adopted the 5%-offset diameter method (ASTM 2018) as shown in Fig. 6. From the load–displacement relationship, the yield or proportional point ( $P_y$ ) and the ultimate point ( $P_u$ ) can be identified (note:  $P_u$  corresponds to the peak load on the graph). The displacement at  $P_y$  is referred to as  $D_y$ , while  $D_u$  represents the displacement at  $P_u$ .

The moments at the yield load ( $M_y$ ) and at the ultimate load ( $M_u$ ) are calculated by multiplying the corresponding loads,  $P_y$  and  $P_u$  by the distance from the load application point to the center of the connection ( $l$ ). Both  $P_y$  and  $M_y$  are critical indicators of the transition from elastic to post-elastic behavior.

The rotation at the yield load ( $\theta_y$ ) and at the ultimate load ( $\theta_u$ ) are calculated by dividing the corresponding displacements,  $D_y$  and  $D_u$ , by the distance from the load application point to the center of the connection ( $l$ ).

$$K_e = \frac{M_y}{\theta_y} \quad (1)$$

$$K_p = \frac{M_u - M_y}{\theta_u - \theta_y} \quad (2)$$

The ductility ratio ( $\mu$ ) is defined as the ratio of  $D_u$  to  $D_y$  (Eq. 3). Initial rotational stiffness ( $K_e$ ) and post-elastic rotational stiffness ( $K_p$ ) can be calculated using Eqs. 2 and 3, based on the fundamental principles of mechanics of materials (Hibbeler 2023):

$$\mu = \frac{D_u}{D_y} \quad (3)$$

The rotational angle ( $\theta$ ) can be calculated by dividing the displacement ( $D$ ) by the distance from the load point to the center of the connection ( $l$ ). Figure 7 shows the graphic display of angular deformation.

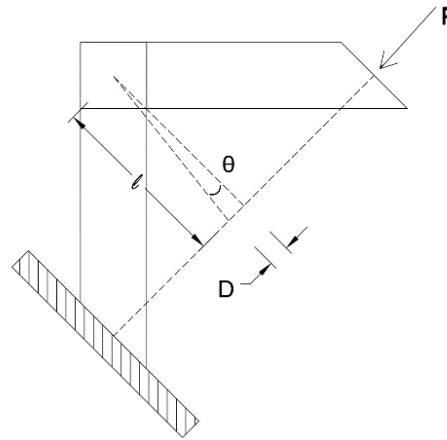


**Fig. 7.** Graphic display of angular deformation

According to CEN (European Committee for Standardisation) the rotational stiffness is calculated from 10% to 40% of the peak or ultimate load (CEN 2005; Mehra *et al.* 2022) using Eq. 4,

$$k = \frac{M_{.40} - M_{.10}}{\theta_{avg,.40} - \theta_{avg,.10}} \quad (4)$$

where  $M_{.10}$  is the moment at the 10% ultimate load,  $M_{.40}$  is the 40% ultimate load,  $\theta_{avg,.10}$  is the rotational angle at  $M_{.10}$ , and  $\theta_{avg,.40}$  is the rotational angle at  $M_{.40}$ . This can be determined by plotting the graph of moment *versus* rotation.

## RESULTS AND DISCUSSION

Figure 8 shows the load-displacement curves of the glulam beam-to-column connections Type 1 and Type 2. The curves illustrate how the connections respond to increasing load, identifying stiffness, yielding, and post-yield behavior. In general, the load-displacement curves for both Type 1 (Fig. 8a) and Type 2 (Fig. 8b) demonstrate similar behavioral pattern. Initially, the load increased steadily, reaching a first peak point, after which a sudden drop in load was observed. This drop likely corresponds to an initial failure mode, such as splitting in the timber, bolt yielding, or local crushing around the bolts. These curves also show a second peak or plateau, indicating the connection could re-engage mechanically (*e.g.*, additional bolts taking load or friction effects). Despite initial damage, the connections do not fail in a brittle manner and maintain considerable residual load capacity, which is a positive sign for structural resilience.

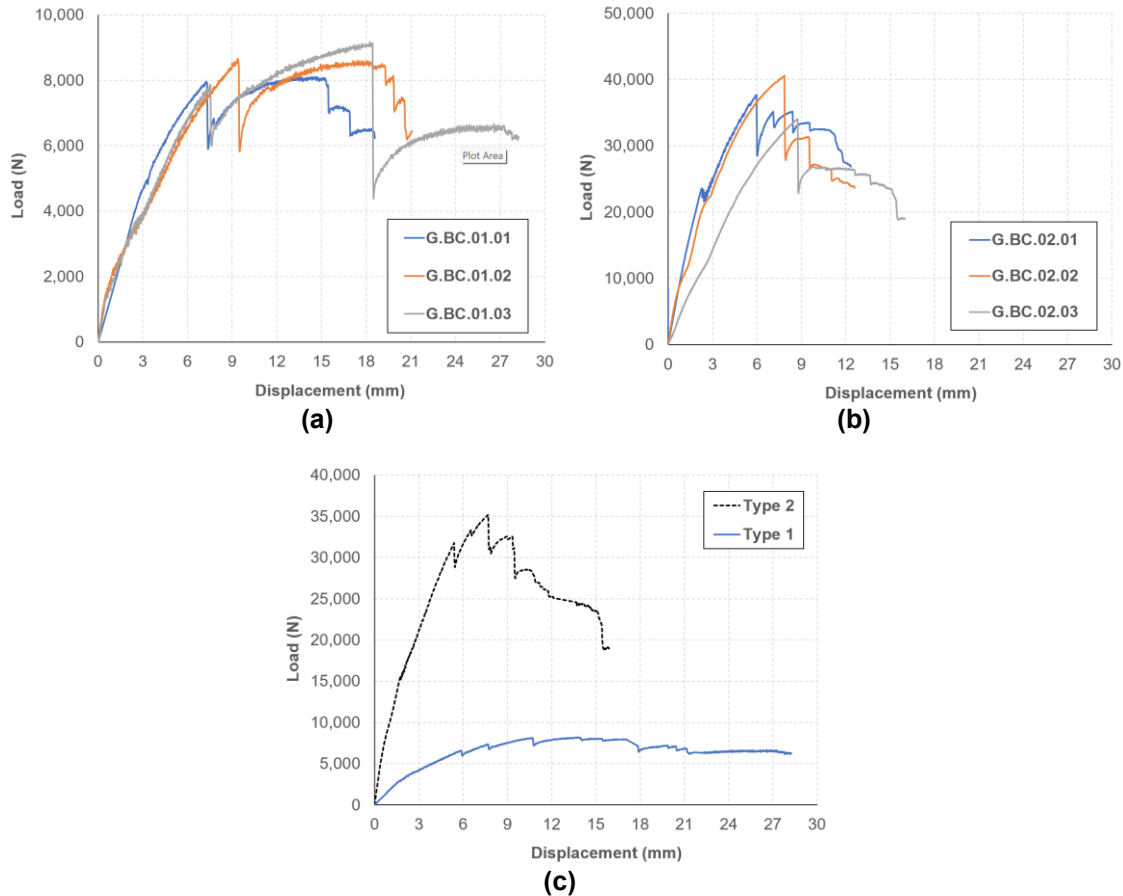


**Fig. 8.** Load-displacement graphs for beam-to-column connections: (a) Type 1, (b) Type 2, and (c) comparison between Type 1 and Type 2

Comparing the graphs for Type 1 and Type 2 (Fig. 8c), both exhibited a steep, nearly linear increase in load at 0 to 6 mm displacement. Type 2 showed a steeper slope than Type 1, indicating higher initial stiffness and load capacity. Type 1 reached a peak load of approximately 8,000 N around 10 mm of displacement, and Type 2 reached the peaks at a much higher load of about 35,000 N around 8 mm of displacement. This indicates that Type 2 connections can sustain more than four times the load compared to Type 1. This increase is likely due to larger cross-sectional dimensions, more bolts, or more laminae (6-lamina glulam) used in Type 2. However, the maximum displacements for Type 1 connection all surpassed 15 mm, showing good ductility ratio compared to Type 2 connection.

The joint properties for both types of connections are presented in Table 2 and Table 3. From Table 2, the proportional load  $P_y$  and the load-carrying capacity  $P_u$  of Type 1 connections were 7340 N and 8640 N, respectively. At the ultimate condition, the ductility ratio was 2.60; therefore, Type 1 connections fell into the low or partial ductility category. Meanwhile, the Type 2 connections exhibited a proportional load ( $P_y$ ) of 33,400 N and a load-carrying capacity ( $P_u$ ) of 37,200 N (see Table 3). These values indicate relatively high initial stiffness and strength. However, at the ultimate condition, the ductility ratio was calculated to be 1.27. Based on this value, Type 2 connections can be classified within the brittle ductility category, indicating limited deformation capacity before failure.

**Table 2.** The Proportional Limit, Load-carrying Capacity and Ductility Ratio of Glulam Beam-to-column Connections for Type 1 and Type 2

Type	Specimen	$P_y$ (N)	$D_y$ (mm)	$P_u$ (N)	$D_u$ (mm)	$\mu$
1	Specimen1	6980.39	5.61	8335.26	15.37	2.74
	Specimen2	7288.45	6.82	8489.37	17.90	2.63
	Specimen3	7761.94	7.48	9105.97	18.23	2.44
	Average	7343.59	6.64	8643.53	17.17	2.60
2	Specimen1	33568.72	6.92	37385.07	8.87	1.28
	Specimen2	36325.05	8.33	40356.32	10.92	1.31
	Specimen3	30393.68	10.11	33994.50	12.36	1.22
	average	33429.15	8.45	37245.30	10.72	1.27

**Table 3.** The Moment Capacity, Rotational Stiffness, Initial Stiffness, and Post-elastic Stiffness of Glulam Beam-to-column Connection Type 1 and Type 2

Type	Specimen	$M_y$ (kN.m)	$\theta_y$ (rad.)	$M_u$ (kN.m)	$\theta_u$ (rad.)	$K_e$ (kN.m/rad)	$K_p$ (kN.m/rad)	$k^*$ (kN.m/rad)
1	Specimen1	3.68	0.0106	4.40	0.0291	347.17	38.92	355.13
	Specimen2	3.85	0.0129	4.48	0.0339	298.45	30.00	342.47
	Specimen3	4.10	0.0142	4.80	0.0346	288.73	34.31	325.94
	Average	3.87	0.0126	4.56	0.0325	311.45	34.41	341.18
2	Specimen1	19.06	0.0122	21.22	0.0156	1562.30	635.29	3135.33
	Specimen2	20.62	0.0147	22.91	0.0192	1402.72	508.89	2514.40
	Specimen3	17.26	0.0178	19.30	0.0218	969.66	510.00	1537.50
	Average	18.98	0.0149	21.15	0.0189	1311.56	551.39	2395.74

Note: \* based on Eq. 4

The mechanical performance of Type 1 and Type 2 connections was evaluated through key parameters, such as yield moment, ultimate moment capacity, and stiffness characteristics, as shown in Table 3. This pronounced stiffness degradation, coupled with a low ductility ratio, classified Type 1 connections as having low or partial ductility. Such behavior indicates limited capacity for inelastic deformation and energy dissipation, raising concerns about their suitability in structures subjected to dynamic or seismic loading.

Type 2 connections showed significantly higher strength and stiffness. Although this still represents a loss in stiffness, it is considerably less severe than that of Type 1 connections. Nevertheless, the ductility ratio for Type 2 was measured at just 1.27, placing it within the brittle category. Although Type 2 connections perform better in terms of post-elastic stiffness and rotational response, their low ductility ratio indicates limited plastic deformation capacity, which could lead to sudden failure under extreme loading.

Figures 9 and 10 illustrate the observed failure patterns of the tested specimens. In both cases, the failure was characterized by a longitudinal split along the bolt line in the column.



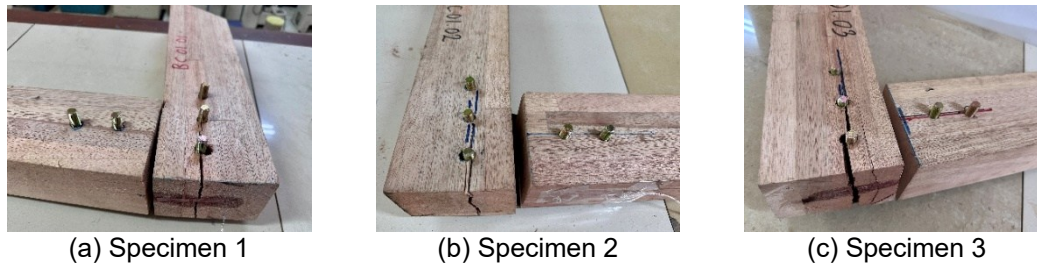


**Fig. 9.** Failure pattern of three specimens of glulam beam-to-column connections Type 1

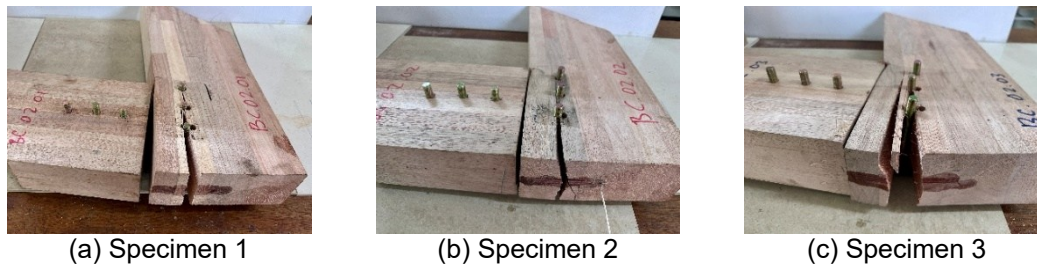


**Fig. 10.** Failure pattern of three specimens of glulam beam-to-column connections Type 2

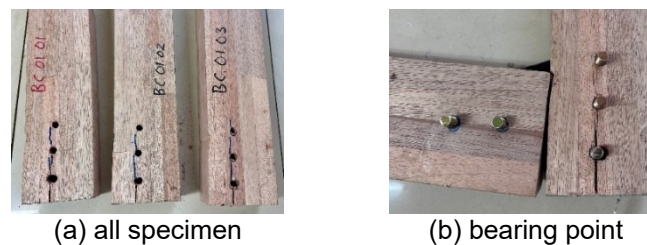


**Fig. 11.** Bearing points on the Type 1 glulam beam-to-column connections

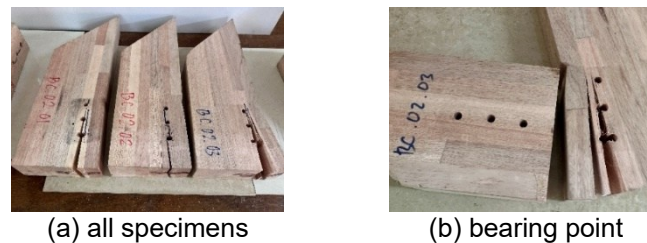


**Fig. 12.** Bearing points on the Type 2 glulam beam-to-column connections

The failure mechanism was initiated at the outermost layer of the beam cross-section, specifically in the region subjected to compressive stress perpendicular to the wood grain at the bearing interface with the column. This initial crushing led to crack propagation along the grain, ultimately resulting in a longitudinal split. The detailed progression of this failure is depicted in Fig. 11 for the Type 1 connection and in Fig. 12 for the Type 2 connection. The Type 2 connection exhibited a more extensive and deeper split that ran through bearing point, with visible widening of the crack.

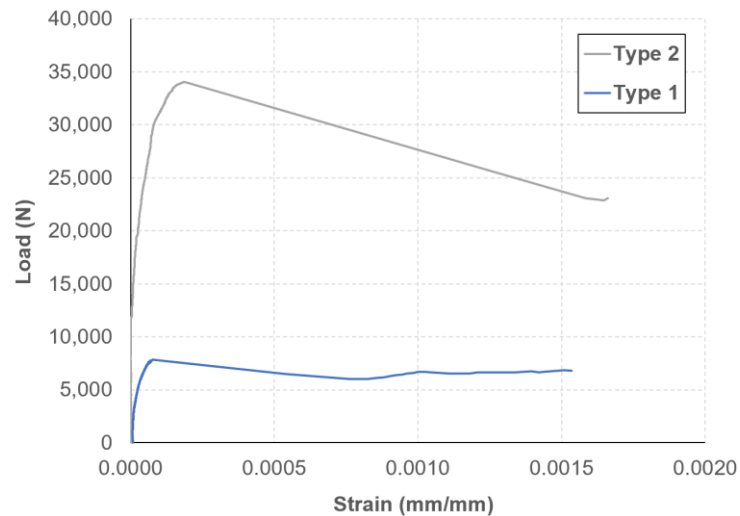


**Fig. 13.** Load and strain relationship obtained for Type 1 and Type 2 connections

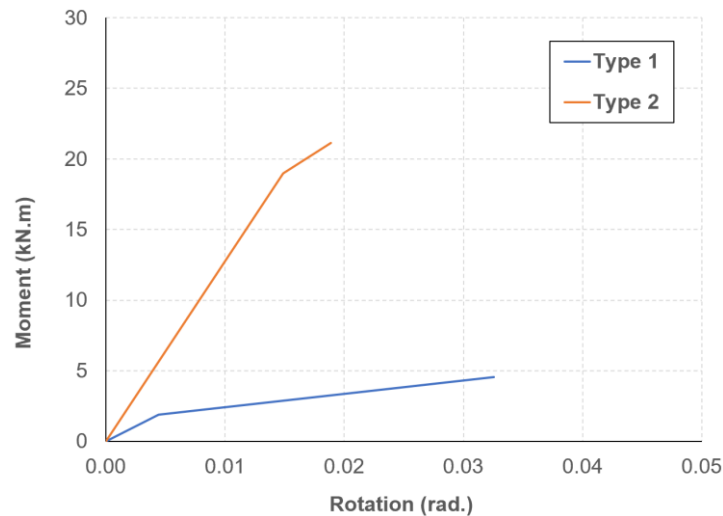


**Fig. 14.** Bilinear model of the moment and rotational relationship of Type 1 and Type 2 connections

Empirical data are shown in Fig. 13 for the Type 1 and Type 2 connections after the maximum load is reached, resulting in a split in the direction parallel to the wood grains in the bolt row in the column. The compressive stress perpendicular to the wood grain caused the wood grain to become compacted so that there was no failure at this bearing point. This can happen because the bearing strength has not been exceeded. The bearing strength parallel to the grain of Meranti Merah wood is 32.7 MPa (Pranata and Suryoatmono 2024), while the stress that occurs in the column at maximum conditions was 20.7 MPa, as shown in Fig. 13, which occurred when the maximum load was 33,400 N (Type 2 Connection), while for Type 1 connections it was much lower. There was a significant change in strain in the outermost layer of the beam cross-section experiencing tensile stress.

Figure 14 shows the bilinear stiffness curve model of the relationship between moment and rotation for the Type 1 and Type 2 glulam beam-column connections. The steel plates had an impact on the behavior of the connection, becoming more ductile. This

was indicated by the failure pattern of the connection, which was split in the column bolts row. This stiffness model can then be used as input data for spring properties of similar connections in the analysis of multi-story building structures. Figure 14 shows that the moment capacity at the elastic rotation connection condition was 19.0 kN.m (Type 2 Connection), while for the Type 1 connection it was 1.88 kN.m. These results can be an alternative reference for nominal moment parameters for structural planners in studying the connection capacity for the same type.

## CONCLUSIONS

This study evaluated the structural performance and failure behavior of two types of glulam beam-to-column connections under monotonic loading. The results indicate that the type 1 connection was in the partial or medium ductility capacity category ( $\mu = 2.60$ ), while the type 2 connection was in the limited ductility ( $\mu = 1.27$ ). The average moment capacities of type 1 and type 2 connections were 4.56 kN.m and 21.2 kN.m, respectively. The moment and rotation relationships models of the glulam beam-column were approximately bilinear with initial stiffness 9 times and 2.4 times for type 1 and type 2 connections, respectively, compared to corresponding post-elastic stiffness.

Despite this superior performance, both connection types exhibited brittle failure patterns, primarily characterized by splitting along the grain in the column bolt row, initiated by tensile stresses in the outermost layer of the beam.

The steel plates had an impact on the behavior of the connection. Steel plates helped improve ductility ratio, as shown by splitting failures near the column bolt rows. This stiffness model can then be used as input data for spring properties of similar connections in the analysis of multi-story building structures.

## ACKNOWLEDGEMENT

This research was funded by Maranatha Christian University, Indonesia, fiscal year of 2025, as an implementation of the collaboration research with Universiti Teknologi MARA (UiTM), Malaysia and Parahyangan Catholic University (UNPAR), Indonesia. This research was also supported by Woodlam Indonesia.

## REFERENCES CITED

- ASTM D5764 (2018). "Standard test method for evaluating dowel-bearing strength of wood and wood-based products," ASTM International, West Conshohocken, PA, USA.
- Amrudin, A. A., Mohamad Bhkari, N., Haris Fadzilah, N. A., Hassan, R., Ahmad, Z., Suryoatmano, B., Tjahjanto, H. H., Wong, N. S. Y., and Azmi, A. (2024). "Effects of bolt diameter and loading direction on bearing and withdrawal resistance of half-threaded bolts in glued laminated timber," *BioResources* 19(4), 9060-9074. DOI: 10.15376/biores.19.4.9060-9074

- EN 26891 (1991). “Timber structures - Joint made with mechanical fasteners - General principles for the determination of strength and deformation characteristics,” European Committee for Standardization, Brussels, Belgium.
- EN 12512:2001/A1:2005 (2005). “Timber structures - Test methods - Cyclic testing of joints made with mechanical fasteners,” European Committee for Standardization Brussels, Belgium.
- Furuheim, E. F., and Nesse, P. M. (2020). *Beam-Column Connections in Glulam Structures, with Gusset Plates of Birch Plywood and Self-Tapping Screws*, Master’s Thesis, Faculty of Science and Technology, Norwegian University of Life Sciences, As, Norway.
- He, M., Li, M., Li, Z., He, G., and Sun, Y. (2021). “Mechanical performance of glulam beam-to-column connections with coach screws as fasteners,” *Archives of Civil and Mechanical Engineering* 21, article 207. DOI: 10.1007/s43452-021-00207-5
- He, M., Luo, J., Tao, D., Li, Z., Sun, Y., and He, G. (2020). “Rotational behavior of bolted glulam beam-to-column connections with knee brace,” *Engineering Structures* 207, article ID 110251. DOI: 10.1016/j.engstruct.2020.110251
- Hibbeler, R. C. (2023). *Mechanics of Materials 11<sup>th</sup> Edition*, Pearson Prentice Hall, Upper Saddle River, NJ, USA.
- Hubbard, C., and Salem, O. (2024). “A new moment-resisting glulam beam-end connection utilizing mechanically fastened steel rods – An experimental study,” *Applied Mechanics* 5, 260-279. DOI: 10.3390/applmech5020016
- Li, Z., Feng, W., Ou, J., Liang, F., and He, M. (2021). “Experimental investigations into the mechanical performance of glulam dowel-type connections with either bolts or screws as fasteners,” *Journal of Wood Science* 67, 71-82. DOI: 10.1186/s10086-021-02002-5
- Mehra, S., O’Ceallaigh, C., Sotayo, A., Guan, Z., and Harte, A. M. (2022). “Experimental investigation of the moment-rotation behavior of beam-column connections produced using compressed wood connectors,” *Construction and Building Materials* 331, article ID 127327. DOI: 10.1016/j.conbuildmat.2022.127327
- Murtopo, A., Jannah, R. M., Sabila, and Tsaniyah, L. (2020). “Failure analysis of glulam lumber beam made from meranti lumber pieces (*Shorea* sp.),” *Jurnal Teknik Sipil dan Perencanaan* 22(2), 137-145. DOI: 10.15294/jtsp.v22i2.26231
- Ottenhaus, L.-M., Jockwer, R., van Drimmelen, D., and Crews, K. (2021). “Designing timber connections for ductility – A review and discussion,” *Construction and Building Materials* 304, article ID 124621. DOI: 10.1016/j.conbuildmat.2021.124621
- Pozza, L., D’Amato, G., Brugnara, P., Callegari, E., and Sestigiani, L. (2023). “Experimental and analytical analysis of timber connections with interposed acoustic resilient strip,” in: *World Conference on Timber Engineering (WCTE 2023)*, Oslo, Norway, pp. 1330-1335. DOI: 10.52202/069179-0181
- Pranata, Y. A. (2011). *Flexural Behavior of Indonesian Timber Bolt-laminated Beams*, Ph.D Dissertation [in Indonesian], Parahyangan Catholic University, Bandung, Indonesia.
- Pranata, Y. A., Pattipawaej, O. C., and Setiadi, A. (2024). “Beam-column and beam-beam joints for earthquake-resistant wooden houses” [in Indonesian], Final Report of Regular Fundamental Research of National Competitive Research, Ministry of Education, Culture, Research and Technology, Indonesia.
- Pranata, Y. A., Pattipawaej, O. C., and Ahmad, Z. (2025a). *Behavior of Beam-to-column Joint of Laminated-Veneer-Lumber (LVL) Using T-Plates*, Research Report of

Internal Scheme, Faculty of Smart Technology and Engineering, Maranatha Christian University, Bandung, Indonesia.

- Pranata, Y. A., Pattipawaej, O. C., and Setiadi, A. (2025b). "Effect of diameter and number of bolts on the rotation stiffness of beam-to-column timber joints," *Journal of Building Material Science* 7(2), 97-110. DOI:10.30564/jbms.v7i2.9704
- Pranata, Y. A., and Suryoatmono, B. (2024). "Experimental tests of red meranti (*shorea* spp.) Dowel bearing strength at an angle to the grain," *Wood Research* 69(3), 369-375, DOI: 10.37763/wr.1336-4561/69.3.369375
- Pranata, Y. A., Suryoatmono, B., and Tjondro, J. A. (2013). "Experimental research on yield bending strength ( $F_{yb}$ ) of bolts [in Indonesian], *Jurnal Teknik Sipil* 12(2), 98-103. DOI: 10.24002/jts.v12i2.607
- Reboucas, A. S., Mehdipour, Z., Branco, J. M., and Lourenço, P. B. (2022). "Ductile moment-resisting timber connections: A review," *Buildings* 12(2), article 240. DOI: 10.3390/buildings12020240
- Swedish Wood (2024a). *The Glulam Handbook Volume 1*, Swedish Wood, Stockholm, Sweden.
- Swedish Wood (2024b). *The Glulam Handbook Volume 2*, Swedish Wood, Stockholm, Sweden.
- Yang, D., Xu, M., and Chen, Z. (2021a). "Seismic performance of Chinese traditional timber frames," *BioResources* 16(3), 6135-6146. DOI: 10.15376/biores.16.3.6135-6146
- Yang, H., Wang, C., Hu, J., Tao, H., Liu, J., Tang, L., and Shi, B. (2021b). "Experimental static and seismic behavior of glulam beam-to-column connection with screwed-in threaded rod joints," *BioResources* 16(3), 5272-5286. DOI: 10.15376/biores.16.3.5272-5286

Article submitted: May 13, 2025; Peer review completed: June 14, 2025; Revised version received: July 28, 2025; Accepted: July 29, 2025; Published: August 7, 2025.  
DOI: 10.15376/biores.20.4.8551-8565